

AD \_\_\_\_\_

Award Number: DAMD17-01-1-0435

TITLE: Optimization of breast cancer treatment by dynamic  
intensity modulated electron radiotherapy

PRINCIPAL INVESTIGATOR: Dennis D. Leavitt, Ph.D.  
David K. Gaffney, M.D., Ph.D.

CONTRACTING ORGANIZATION: University of Utah  
Salt Lake City, Utah 84102-1870

REPORT DATE: October 2002

TYPE OF REPORT: Annual

PREPARED FOR: U.S. Army Medical Research and Materiel Command  
Fort Detrick, Maryland 21702-5012

DISTRIBUTION STATEMENT: Approved for Public Release;  
Distribution Unlimited

The views, opinions and/or findings contained in this report are  
those of the author(s) and should not be construed as an official  
Department of the Army position, policy or decision unless so  
designated by other documentation.

20030328 253

**REPORT DOCUMENTATION PAGE**Form Approved  
OMB No. 074-0188

maintaining  
the data needed, and completing and reviewing this collection of information. Send comments regarding this burden estimate or any other aspect of this collection of information, including suggestions for reducing this burden to Washington Headquarters Services, Directorate for Information Operations and Reports, 1215 Jefferson Davis Highway, Suite 1204, Arlington, VA 22202-4302, and to the Office of Management and Budget, Paperwork Reduction Project (0704-0188), Washington, DC 20503

**1. AGENCY USE ONLY (Leave blank)****2. REPORT DATE**  
October 2002**3. REPORT TYPE AND DATES COVERED**

Annual (1 Oct 2001 - 30 Sep 2002)

**4. TITLE AND SUBTITLE**

Optimization of breast cancer treatment by dynamic intensity modulated electron radiotherapy

**5. FUNDING NUMBER**  
DAMD17-01-1-0435**6. AUTHOR(S)**Dennis D. Leavitt, Ph.D.  
David K. Gaffney, M.D., Ph.D.**7. PERFORMING ORGANIZATION NAME(S) AND ADDRESS(ES)**University of Utah  
Salt Lake City, Utah 84102-1870

email dennis.d.leavitt@hsc.utah.edu

**8. PERFORMING ORGANIZATION  
REPORT NUMBER****9. SPONSORING / MONITORING AGENCY NAME(S) AND ADDRESS(ES)**U.S. Army Medical Research and Materiel Command  
Fort Detrick, Maryland 21702-5012**10. SPONSORING / MONITORING  
AGENCY REPORT NUMBER****11. SUPPLEMENTARY NOTES****12a. DISTRIBUTION / AVAILABILITY STATEMENT**

Approved for Public Release; Distribution Unlimited

**12b. DISTRIBUTION CODE****13. ABSTRACT (Maximum 200 Words)**

Three specific work projects were pursued during the first year of this grant:

- 1) Static electron fields defined by the photon MLC were measured. Beam profiles and output factors at distances of 75, 85 and 100 cm SSD were measured for fields from 1 cm to 20 cm wide. Measurements were made for electron energies of 6, 9, 12, 16 and 20 MeV. Profiles were compared vs. energy, and their departure from strictly divergent fields was noted. Profiles defined by the MLC were compared with previous profiles defined by cerrobend™ apertures.
- 2) Monte Carlo techniques were applied to 3D electron dose calculations. The rounded shape of the MLC ends, the long air scatter column, and the reduced density air at Utah altitude were addressed in the calculations. Excellent agreement was achieved compared to measured profiles and measured relative output factors. The Monte Carlo calculations correctly account for air scatter effects vs. field size and SSD, and correctly predict relative output factors vs. field size and SSD.
- 3) An iterative optimization technique to determine the required MLC leaf positions vs. arc rotation was defined. The work to date is on track for successful completion of the project within the grant period.

**14. SUBJECT TERMS**

electron arc therapy, optimization

**15. NUMBER OF PAGES**  
22**16. PRICE CODE****17. SECURITY CLASSIFICATION  
OF REPORT** Unclassified  
Unclassified**18. SECURITY CLASSIFICATION  
OF THIS PAGE** Unclassified  
Unclassified**19. SECURITY CLASSIFICATION  
OF ABSTRACT** Unclassified  
Unclassified**20. LIMITATION OF ABSTRACT**  
Unlimited

## Table of Contents

Cover.....	1
SF298.....	2
Introduction.....	4
Body.....	4
Key Research Accomplishments.....	22
Reportable Outcomes.....	22
Conclusions.....	22
References.....	None
Appendices.....	None

## INTRODUCTION

**Subject:** Electron Arc Therapy was developed to treat extended superficial volumes within the postmastectomy chest wall. This provides an alternative to tangential photon irradiation and offers the potential advantages of greater dose uniformity throughout the prescribed treatment volume, reduced dose to the heart and lungs, and reduced dose to the apex of the lung typically treated using a photon supraclavicular boost field. The primary limitation of this work is the labor-intensive nature of the entire process: Doses are calculated using a simple tabular model; the electron aperture design is determined empirically by repeated estimates of the required shape; and the field edge blocking on the patient is prepared manually. These steps are all labor intensive and depend vitally on the skills of the physicist and dosimetrist. **Purpose:** The current work will overcome these limitations through the introduction of **Intensity Modulated Electron Radiotherapy (IMERT)**. In a manner similar to photon-based static IMRT, IMERT will define the dynamically varying shape of the electron aperture (Multi-Leaf Collimator) as the linear accelerator gantry rotates around the patient and will set up the MLC treatment files required to deliver the optimized dose distribution. This will refine the treatment planning and dose delivery process, and will eliminate the labor-intensive requirements for secondary and tertiary electron collimation. **Scope:** This work will develop advanced 3-dimensional dose calculation algorithms and electron inverse planning optimization; will measure the dose characteristics of electron beams defined by MLC; will confirm the efficacy of dose calculations using phantoms simulating actual patient shape; will evaluate treatment planning Dose Volume Histograms (DVH) comparing IMERT vs. other chest wall radiotherapy techniques; and will test clinical applicability. This is a prospective, evaluative, technical development study that will not involve actual treatment of patients during the period of the work.

## BODY

Two tasks are listed in the statement of work for the first year:

1. Implement a 3-dimensional dose calculation model for inverse planning optimization.
  - a. Dose calculation algorithm development;
  - b. Define electron inverse planning optimization.
2. Measure dose characteristics of electron beams defined by Multi-Leaf Collimator (MLC). (To commence in year one and continue into year two.)
  - a. Static field size measurements;
  - b. Dynamic Multi-Leaf Collimator measurement;
  - c. Dose determination on sloping surfaces.

The development of electron arc therapy preceded the commercial availability of Multi-Leaf-Collimators and sophisticated dose calculation algorithms. Electron arc therapy was therefore constrained to simple two-dimensional tabular dose calculation algorithms supplemented by tables of empirical "correction factors", coupled with manually-cast secondary and tertiary electron field shaping devices. The arrival of commercial MLC's and relatively user-friendly Monte Carlo dose calculation algorithms have enabled this effort to develop a second-generation electron arc therapy capability that can utilize dynamic MLC motion and sophisticated dose calculation within the framework of **Intensity Modulated Electron Radiotherapy (IMERT)**. This work utilizes the **Varian Clinac 2100CD™** with an 80-Leaf MLC and the Monte Carlo code **BEAM-NRC** and **DOSEXYZ** from the Canadian National Research Council.

A key difference of electron arc therapy from standard fixed electron therapy is the distance from the last collimating device to the patient. In standard electron therapy, the collimating aperture ("cone") is

typically positioned only five cm above the patient. In electron arc therapy, the collimating aperture is the MLC located 50 cm above isocenter. This introduces an air gap of 25 cm to 95 cm, corresponding to isocenter depths within a patient of from 25 cm to 5 cm. This is illustrated in Figure 1. The electron profiles are therefore very diffuse, compared to the standard fixed electron profiles. **Static field size measurements** of these electron profiles were made to determine the dosimetric characteristics of the electron fields defined by the MLC. The static field electron dose distributions were measured in the following manner:

1. Primary Photon Jaws were set to 20 cm wide ( X-Jaws in direction of motion of the MLC leaves) by 40 cm long ( Y-Jaws perpendicular to direction of motion of MLC leaves) and were held fixed during all measurements.
2. MLC leaves were set to define field widths from 1 cm wide to 20 cm wide.
3. A Scanditronix water phantom was positioned to scan the electron beam profiles and central axis depth doses at Source-Surface-Distances (SSD) of 75 cm, 85 cm, and 100 cm sequentially.
4. A Scanditronix electron diode was driven in the water phantom to scan the electron profiles at several depths below the water surface. These depths included 1 mm below the surface, depth of maximum buildup ( $d_{max}$ ), and several more depths extending beyond the range of the electrons. A vertical depth dose scan was also included.
5. Beam profile and depth dose measurements were repeated for the full range of field widths and at the three listed SSD's.
6. Measurements were repeated for the five available electron energies: 6, 9, 12, 16 and 20 MeV.
7. All data was entered into the treatment planning data files for our existing two-dimensional treatment planning system.

Representative central axis depth dose curves for 6 MeV and 16 MeV are illustrated in figure 2. 6 and 9 MeV electrons are customarily used for the chest wall, while 12, 16 or 20 MeV electrons are customarily applied to the Internal Mammary Chain where a greater treatment depth is desired.

Representative beam profiles are displayed for 6 MeV and 16 MeV at 85 cm SSD in figures 3 and 4. These profiles illustrate that the lower energy distributions are much more diffuse than are the higher energy distributions. This is demonstrated in the following graphs. The light field on the Varian linear accelerators projects a field diverging from the photon source 100 cm above isocenter. However, the dominant electron source is the electron scattering foil located 88 cm above isocenter. ( This statement must be qualified by acknowledging that additional diffuse effective electron sources that model electron scattering from primary photon jaws and other secondary collimation in the beamline can be included in models.) This difference between light field and actual projected electron field is very small for standard electron applicators where the last aperture is 5 cm above the patient; however, for this application where the last aperture is 50 cm above isocenter the projected field width is wider. This is illustrated in figure 5. Here the projected field width is plotted vs. SSD for light field widths of 3 cm, 5 cm and 7 cm. As noted, all three converge to the location of the electron scattering foil. Superimposed on these projected widths are the measured field widths for 6 MeV at 75 SSD, 85 SSD and 100 SSD. Note that for all three widths the measured profiles diverge from the projected field widths, with the greatest divergence seen for the narrow field. This demonstrates the extreme importance of electron scatter in air in any calculation of electron arc therapy. In figure 6, the 16 MeV beam profile data is superimposed with the 6 MeV data and the projected field widths. The 16 MeV data appear to converge more closely to the projected field width, indicating the smaller influence of air scattering at the higher electron energies.



The influence of location of the final collimating aperture is demonstrated in this paragraph. In work done before the installation of the Varian 80-leaf MLC, the electron arc aperture was formed of cerrobend™ and was positioned in the accessory tray at 65 cm below the photon target (35 cm above isocenter). Figures 7 and 8 compare the beam profiles at 85 cm SSD for light field widths of 3, 5 and 7 cm. They illustrate that there is a greater diffuseness to the profiles defined by the MLC. This illustrates two effects: first, the cerrobend™ aperture is positioned 15 cm closer to the measurement plane, thereby reducing the effects of air scatter; second, the leaves of the MLC are 6 cm thick and are rounded (see figure 1), while the cerrobend™ aperture is one cm thick with straight edges, thereby resulting in less diffuse scatter from the cerrobend™ compared to the MLC. The effect of collimator position and edge shape is again illustrated in figures 9 and 10. The beam profile width for each aperture type is plotted vs. light field width. This illustrates that the beam profiles defined by the MLC diverge greatly from the effective projected field width and finally begin to approach the effective projected field width only for the larger fields, while the profiles defined by the cerrobend™ aperture more closely follow the projected field width. This is shown for both the 6 MeV and the 16 MeV electrons.

A second key difference between electron arc therapy and standard fixed electron therapy is that electron arc therapy is an **isocentric** setup, while fixed electron therapy is an **SSD** setup. Thus, the effective SSD used during an electron arc can vary widely depending on the radius of curvature of the patient. This requires that the dependence of dose rate on effective SSD, i.e., the depth of isocenter, be explicitly calculable. Therefore, the variation in relative output was measured for a range of field widths defined by the MLC from 1 cm wide to 20 cm wide for SSD's of 75 cm, 85 cm and 100cm. These values for 6 MeV electrons are displayed in figure 11 as graphs of the relative output factor vs. MLC field width, with the curve for each SSD normalized to 100% for the 20 cm wide field. The significance of this graph is the following: The effect of the extended air column between the last collimating device (the MLC) and the patient is dramatic, in that the air scattering within this column changes the relative output vs. field width. For example, there is a 15% difference in the relative output (normalized to the 20 cm wide field) between 75 SSD and 100 SSD. These effects must be calculated correctly in order for the electron arc therapy calculations to be valid.

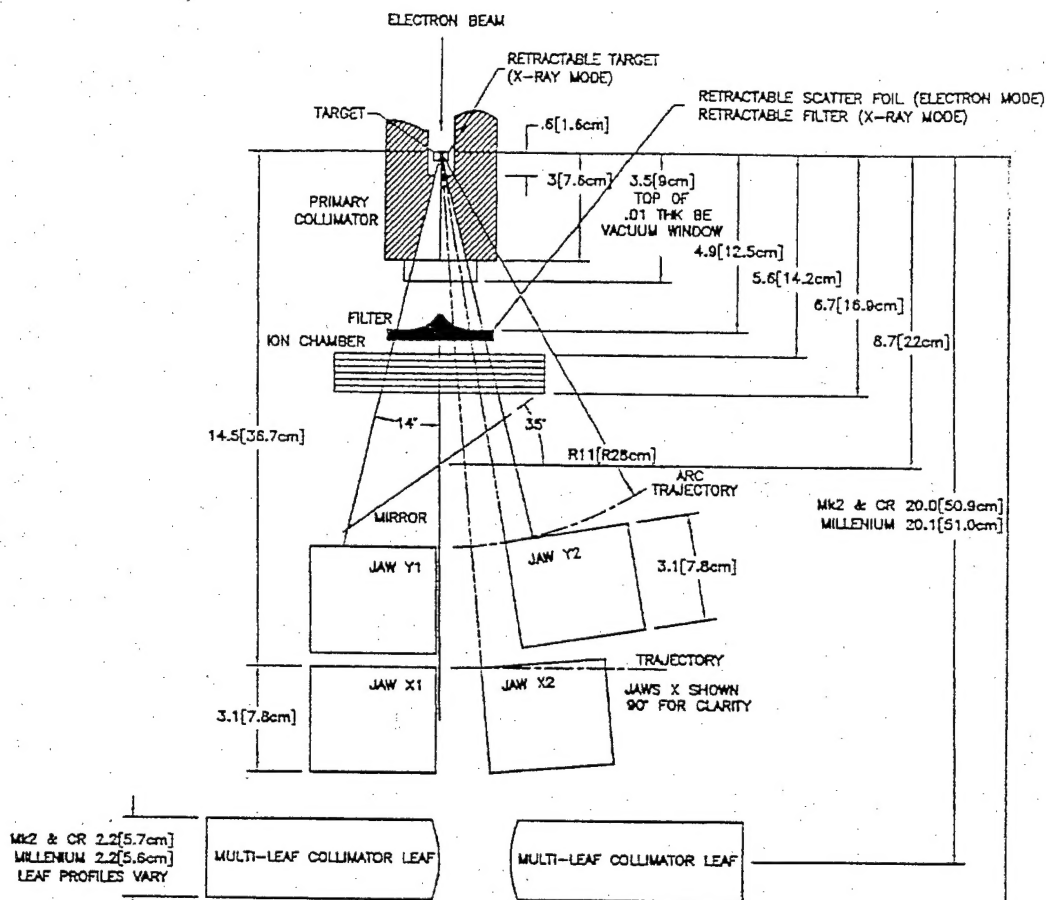
The development of a **three-dimensional electron dose calculation model** is crucial to the success of the electron arc therapy IMERT project. Recent progress in development of efficient Monte Carlo codes for electron dose calculation encouraged our evaluation of such code. The Monte Carlo code BEAMNRC and DOSEXYZ (Canadian National Research Council) has been implemented at our institution specifically to calculate electron arc therapy doses. The key differences from other implementations of Monte Carlo code for electron dose calculations are that the last collimation is 50 cm above isocenter, compared to the more customary 5 cm, and that the collimating device is the photon MLC, rather than a customary electron applicator with cerrobend™ insert. This photon MLC is not ideal for electron collimation, since it is 6 cm thick and has rounded ends on each leaf. The leaf thickness and the rounded ends contribute to increased scatter off the collimator, thereby creating a more diffuse electron profile. The calculation of the electron fluence incident on the phantom depends critically on the correct characterization of all elements in the beamline. Thus, using information provided by Varian, the beamline was characterized to include the primary collimator, the electron scattering foils, the ion chamber, the primary photon jaws and the multileaf collimator. After examination of the open beamline during machine maintenance, the characterization of a secondary collimator between the primary collimator and the scattering foil was added. Additionally, secondary blocking between the ion chamber and the primary photon jaws was characterized.

The results from the Monte Carlo calculations were directly compared against the measured data. Most of the calculation time to date has been directed toward the 6 MeV electrons. The effective energy of the electrons incident on the primary collimator (immediately following the 270 degree bending magnet) was adjusted to 7.6 MeV in order to match the electron depth dose characteristics for the 6 MeV electron beam. This parameter was then held fixed for subsequent dose calculations. Using BEAMNRC and DOSEXYZ, dose profiles were calculated at 75, 85 and 100 cm SSD for a range of field widths up to 20 cm wide. Dose profiles at  $d_{\max}$  (nominally 1.6 cm) were compared with measured dose profiles, and relative output factors were compared with measured values. A key finding is that the dose calculations are particularly sensitive to the density of air through which the electrons transit. Only after the air density was adjusted to account for the reduced air pressure at this altitude was consistent agreement between measurement and calculation achieved. The results are shown in the following illustrations. Figures 12 and 13 compare the Monte Carlo calculated profiles for 3, 5, and 7 cm vs. measured data for 85 and 100 cm SSD. We note that after explicit entry of lower density air, and correct curvature to the MLC leaves the agreement between calculation and measurement is very good. Some differences in the low dose tail of the profile must still be examined.

A critical requirement of the calculations is the ability to predict the relative output vs. field width and SSD. Figure 14 compares the calculated to measured output factors. Again, the agreement is good.

The results of Monte Carlo dose calculations for the 6 MeV data are encouraging. This work will be repeated for the other energies as well. The principal constraint to rapid implementation of this code has been the long calculation times required to achieve adequate statistics. To help alleviate this problem, a parallel array of 25 PC's operating from 2.0 to 2.8 GHz is being purchased using donated funds. This will reduce the calculation time considerably.

The electron inverse planning algorithm differs from both fixed-field photon and electron algorithms. Instead of a rectangular two-dimensional array of diverging pencil beams indexed by position, the electron arc array consists of a two-dimensional array of converging pencil beams indexed by gantry angle and MLC leaf. To minimize the number of dose combinations possible with the MLC settings, the optimization proceeds in an iterative manner. Calculation of dose in the central plane is done first. Then the next superior and inferior planes are optimized. This process is repeated sequentially until all planes have been calculated. This technique for dose optimization mimics our earlier work in which the optimization was done plane-by-plane. Although this may not be possible in a general application, it is successful in the electron arc therapy application since the shape of the electron arc aperture varies smoothly with arc angle and distance superior/inferior. One issue that will influence the efficiency of the optimization process is the extent to which the MLC setting in one plane will influence the dose in neighboring MLC planes. This was investigated in earlier work using a prototype MLC with wider leaves. This investigation will be pursued through measurement and Monte Carlo calculation during the coming year.



100 cm

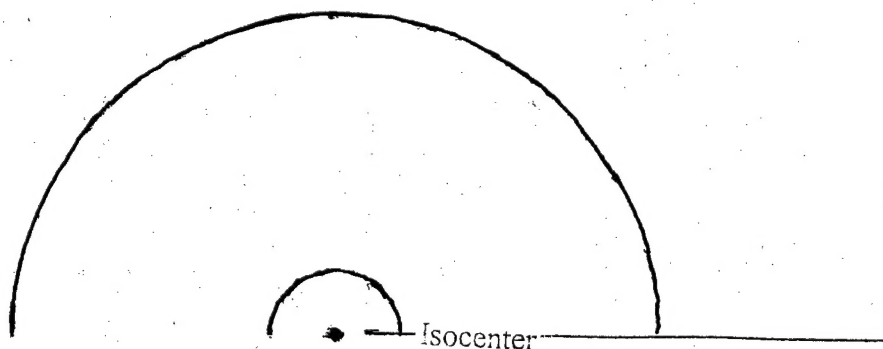


Figure 1: Schematic visualization of beamline for Varian Clinac 2100CD™. Key elements of the beam system are the primary collimator, scattering foils, ionization chamber, primary photon jaws, and multileaf collimator. The elements are shown to scale. The 100 cm to isocenter is also illustrated. The typical range of patient or phantom radius is drawn as 5 cm to 25 cm.



**Central Axis Depth Dose**  
**6 MeV & 16 MeV earc static fields**  
**85 SSD**

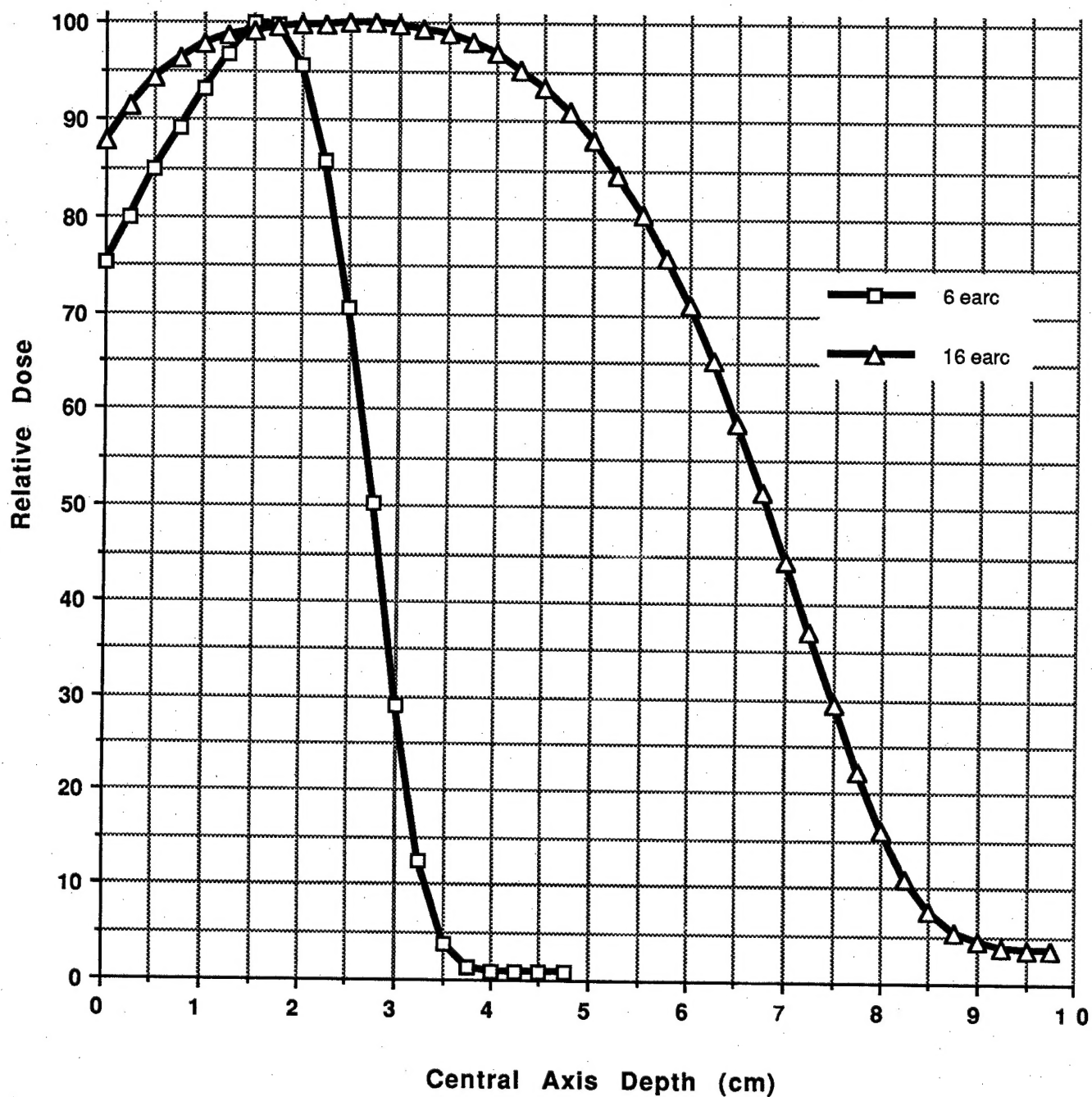


Figure 2: Central axis depth dose curves for 6 MeV (typically applied to lateral chest wall where shallow penetration is desired) and 16 MeV (typically applied to the internal mammary chain where deeper penetration is desired.)

### 6 MeV earc MLC Profiles @ 85 cm SSD

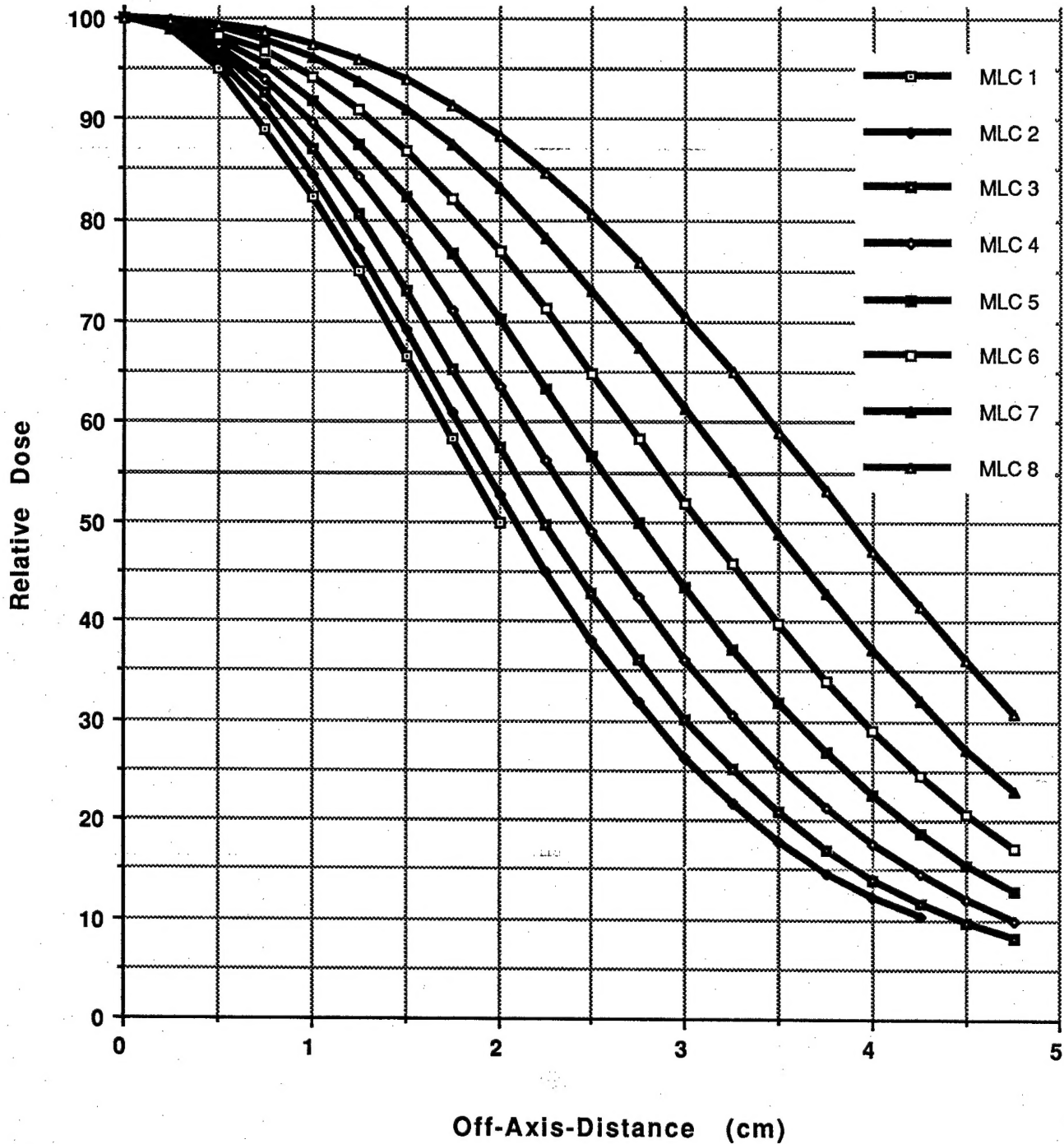


Figure 3: Beam profiles @ $d_{\max}$  depth for 6 MeV electrons measured at 85 cm SSD for light field widths from 1 cm to 8 cm. (The light field width is a console keyboard entry corresponding to the light field projected through the MLC aperture to a distance of 100cm. It is used to reference the field entry. It does not, however, correspond to the actual electron field width, as discussed in the text and following illustrations.)

# 16 MeV earc MLC Profiles @ 85 cm SSD

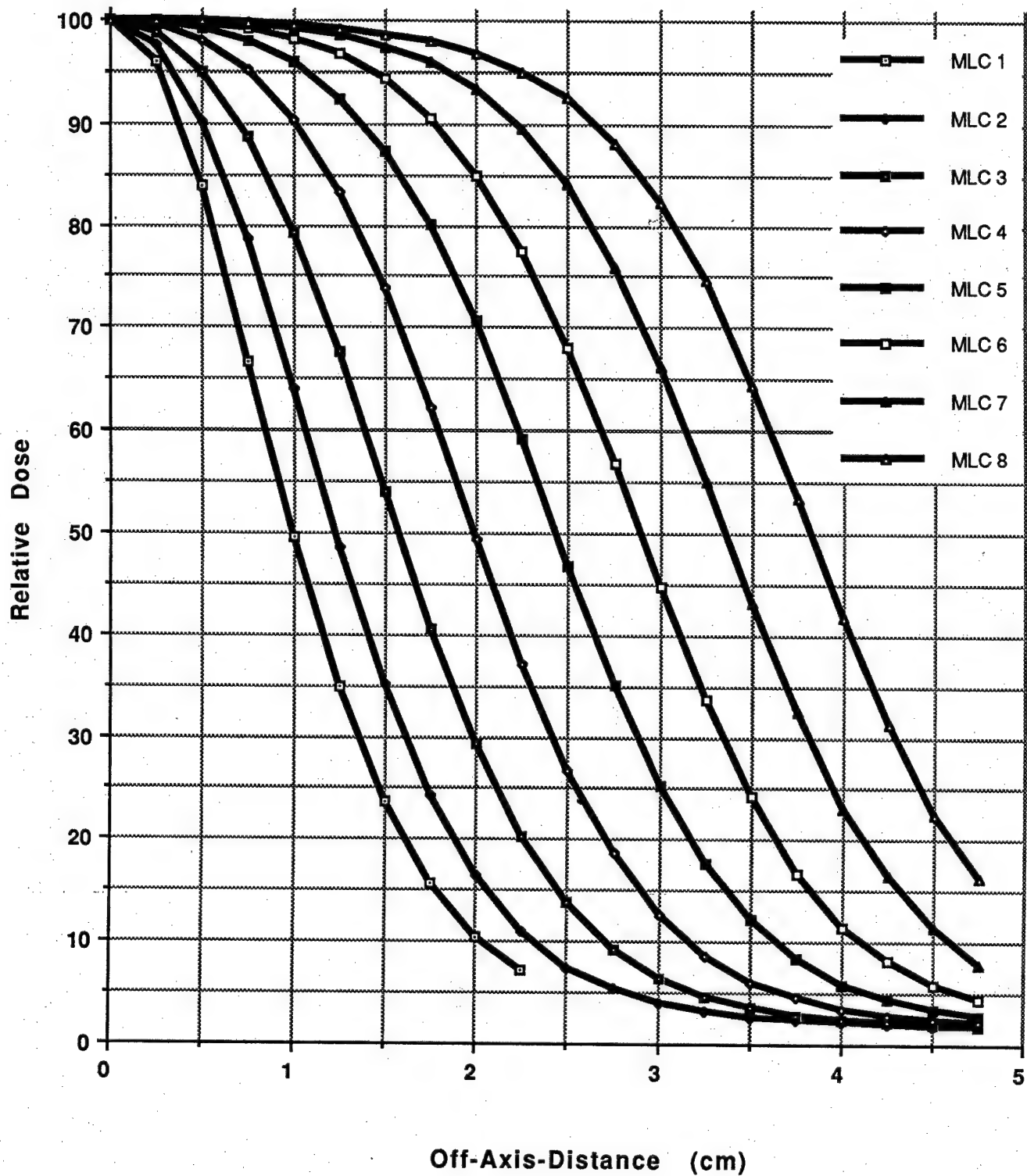


Figure 4: Beam profiles @ $d_{\max}$  depth for 16 MeV electrons measured at 85 cm SSD for light field widths from 1 cm to 8 cm.

## 6 MeV Measured Profiles vs. Projected Field Width vs. Light Field & SSD

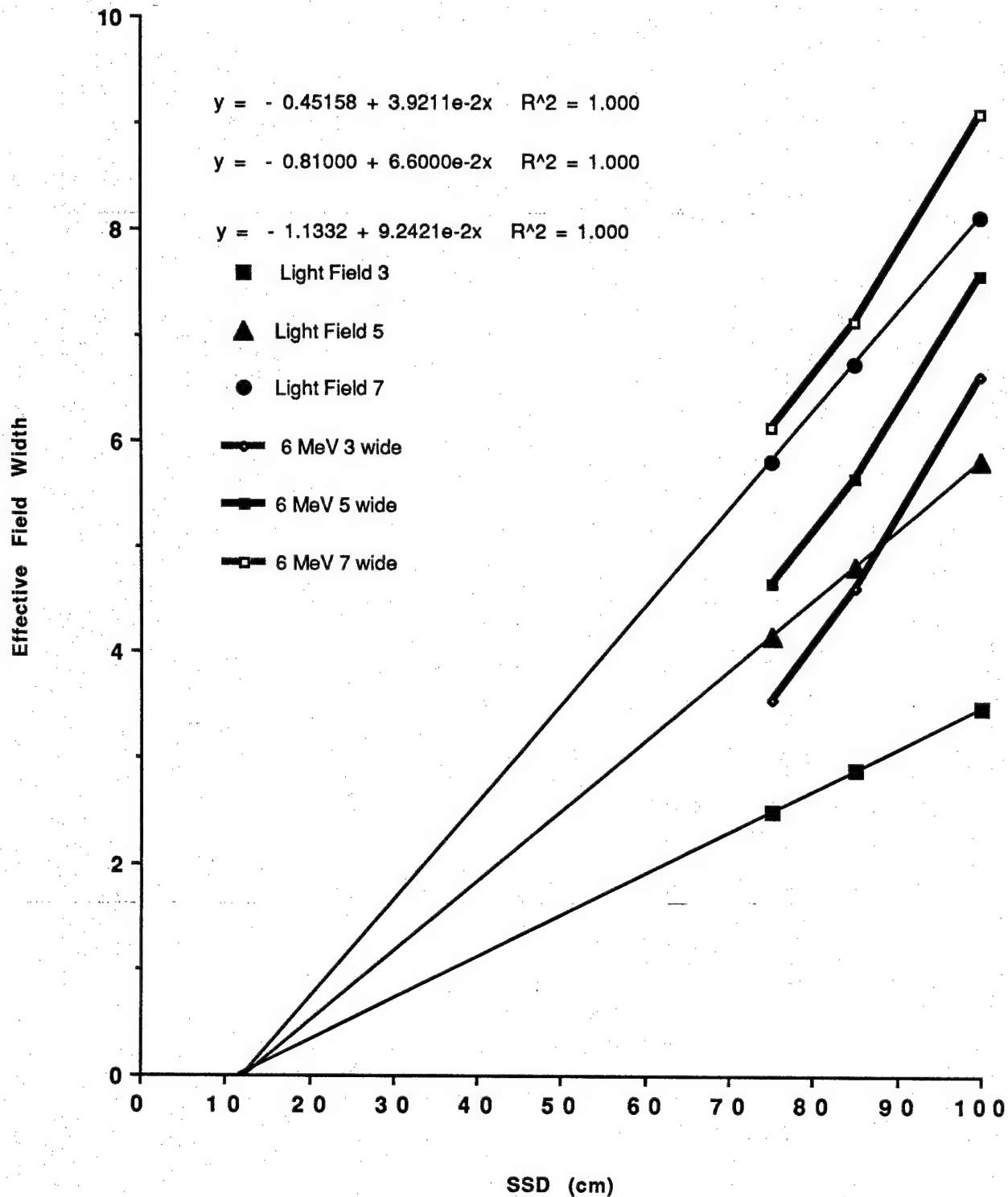


Figure 5: Projected field width from scattering foil through MLC aperture (solid lines converging to 12 cm on x-axis). Measured profiles for 6 MeV electrons are superimposed (solid dark lines extending from 75 cm to 100 cm SSD.) Note that the measured profiles increasingly diverge from the projected field width with increasing SSD. This is attributed to the effects of electron scatter in the air.

## 6 MeV & 16 MeV Measured Profiles vs. Projected Field Width

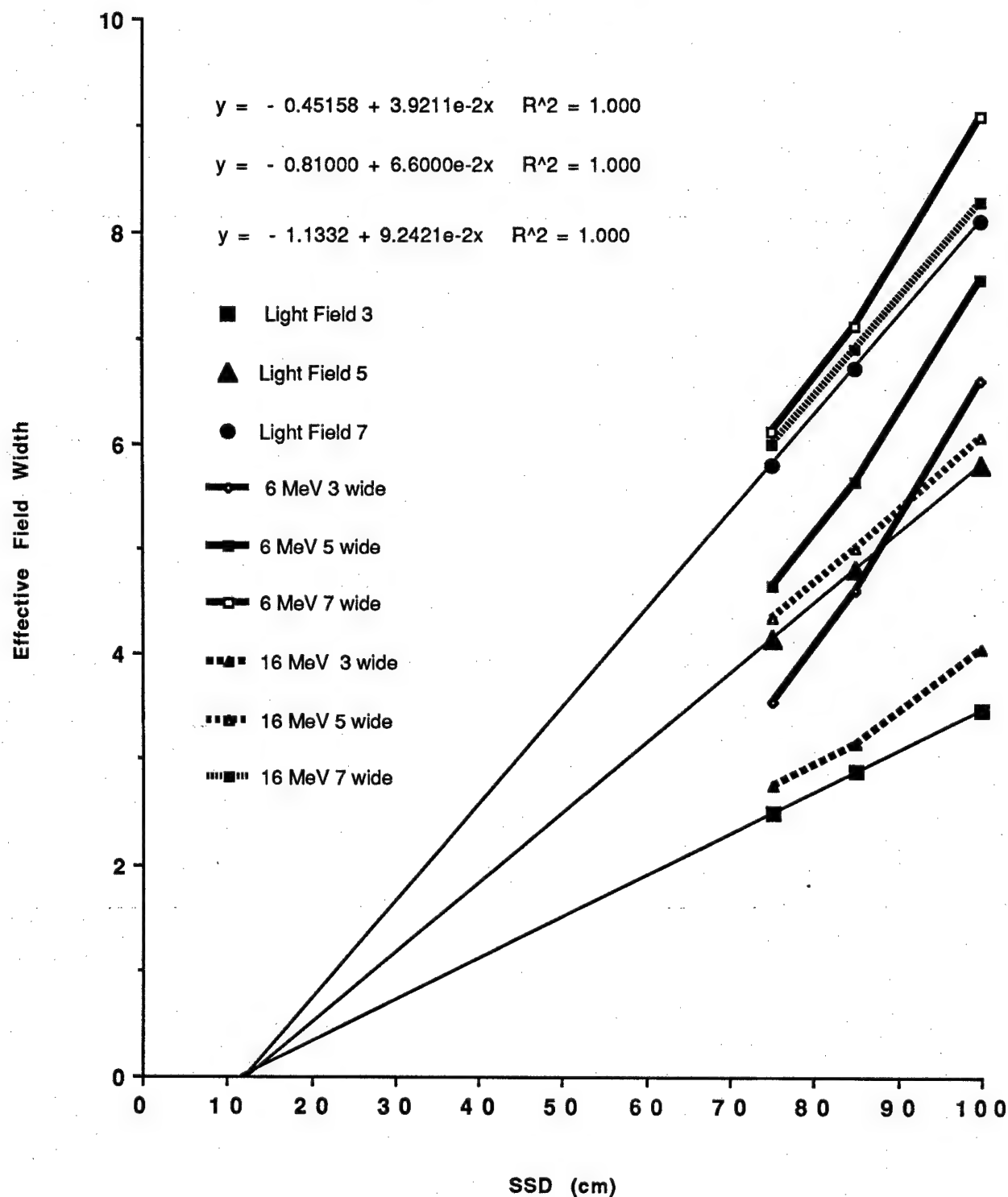


Figure 6: Measured profiles for 16 MeV electrons are superimposed on the previous graph. Note that the profiles corresponding to the higher energy electrons more closely conform to the projected field width.

# 6 MeV earc Profiles @ 85 cm SSD MLC vs Cerrobend Aperture

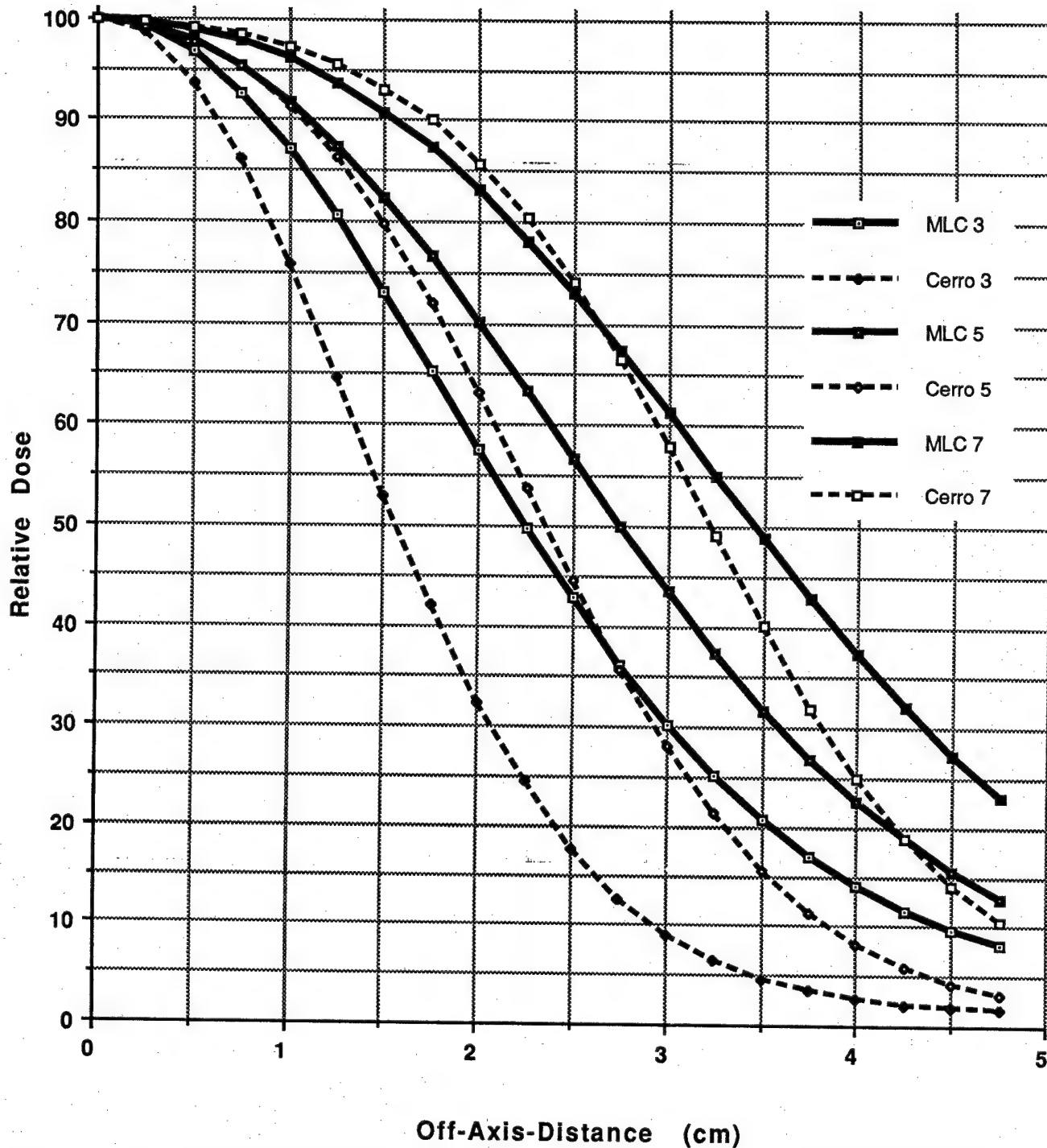


Figure 7: 6 MeV electron profiles are compared for MLC-defined profiles vs. cerrobend<sup>TM</sup>-defined profiles. The difference between the profiles reflects the difference in location of the apertures ( 50.0 cm for the MLC vs. 65 cm for the cerrobend<sup>TM</sup>) and the shape of the collimation ( 6 cm thick with rounded ends for the MLC vs. 1 cm thick with straight edges for the cerrobend<sup>TM</sup>.)



### 16 MeV earc Profiles @ 85 SSD MLC vs Cerrobend Aperture

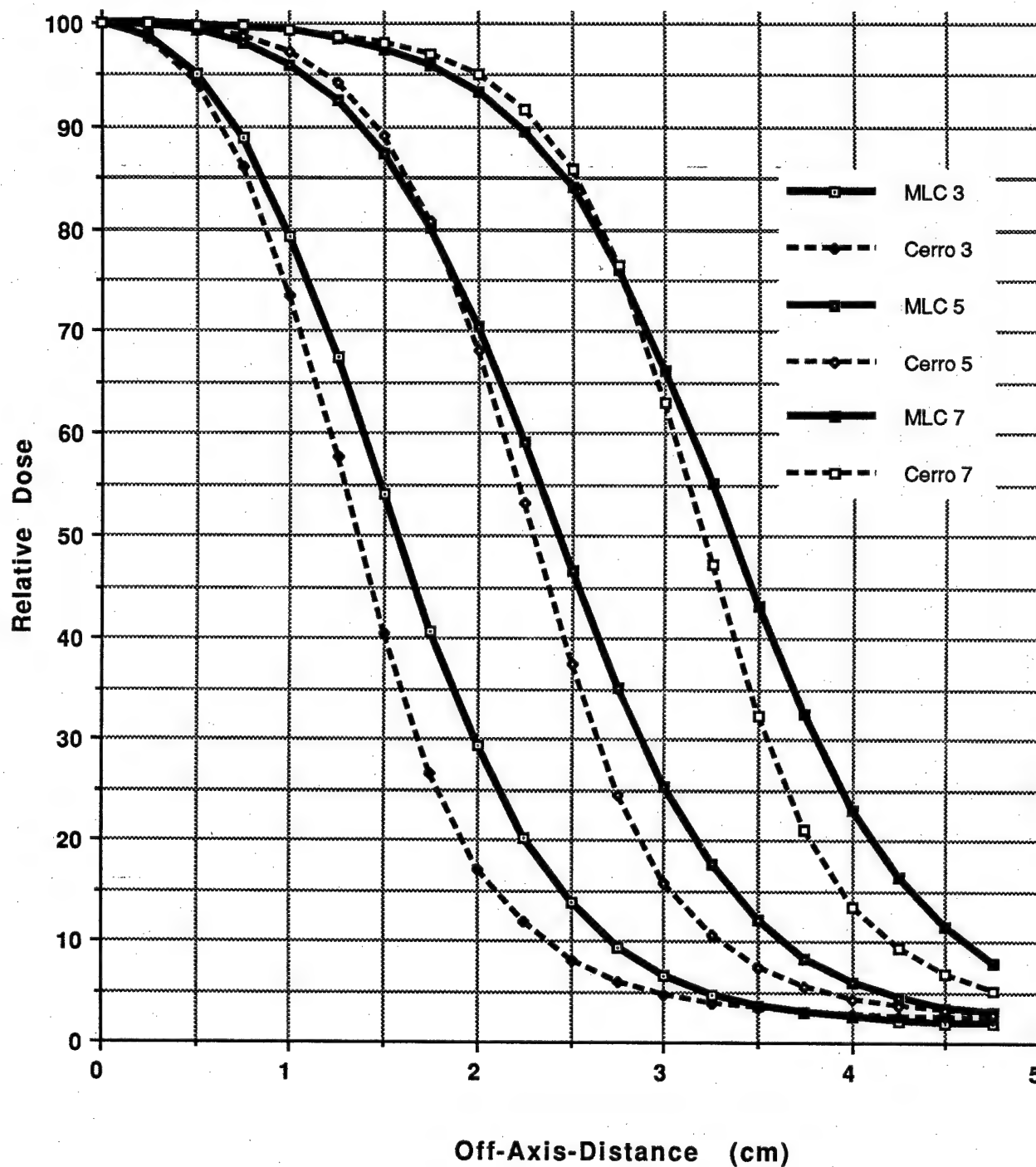


Figure 8: 16 MeV electron profiles are compared for MLC-defined profiles vs. cerrobend<sup>TM</sup>-defined profiles. (See previous figure caption.)

# Full-Width-Half-Maximum @ 85 cm SSD 6 MeV E Arc vs. Light Field Width

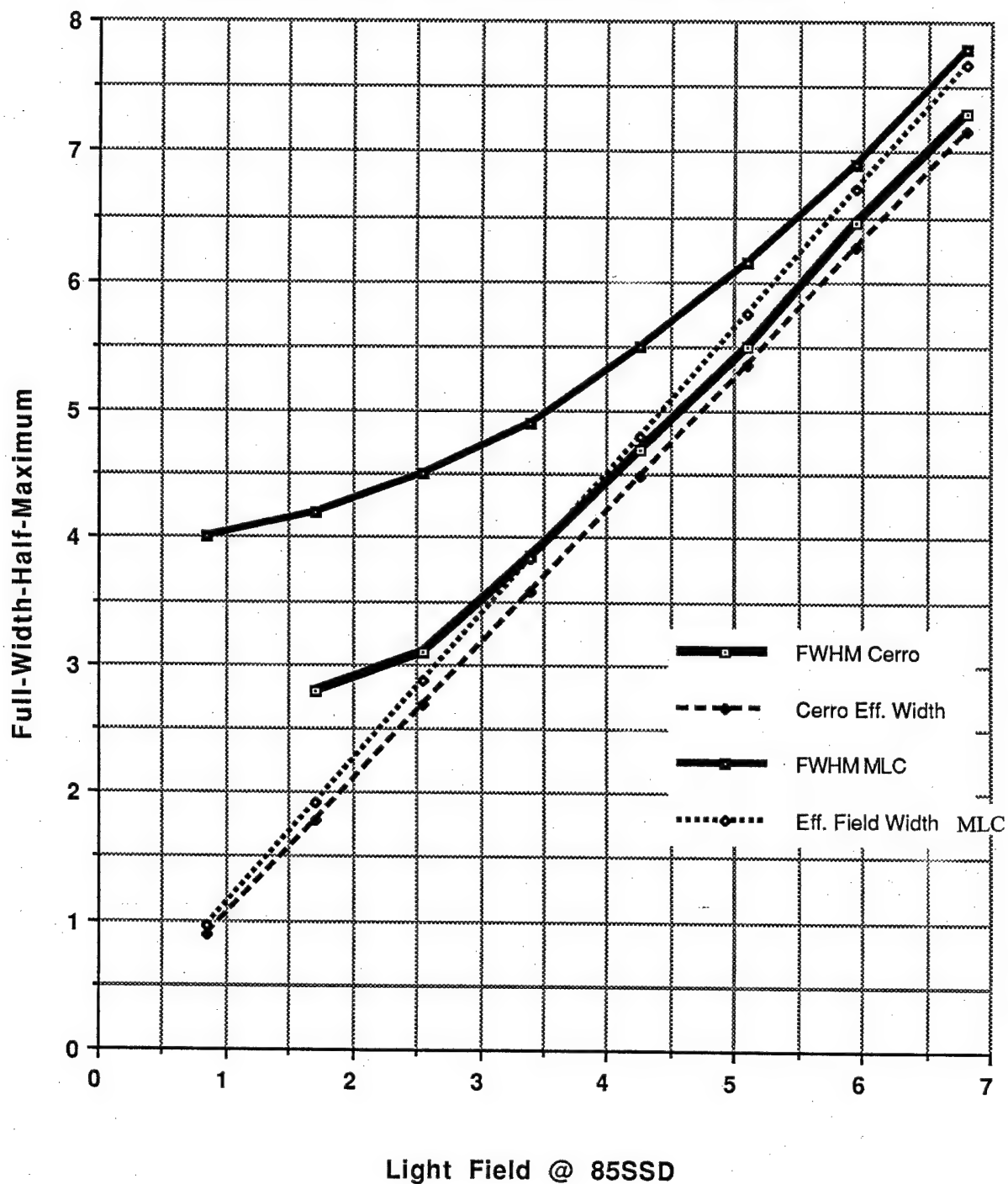


Figure 9: Comparison of 6 MeV beam profiles width vs. light field width @85 cm SSD. MLC profiles are defined by the MLC at 50.9 cm; cerrobend™ profiles are defined by the cerrobend™ aperture at 65 cm. The cerrobend™ profiles converge more rapidly to the effective width projected from the scattering foil.

# **Full-Width-Half-Maximum @ 85 cm SSD** **16 MeV E Arc vs. Light Field Width**

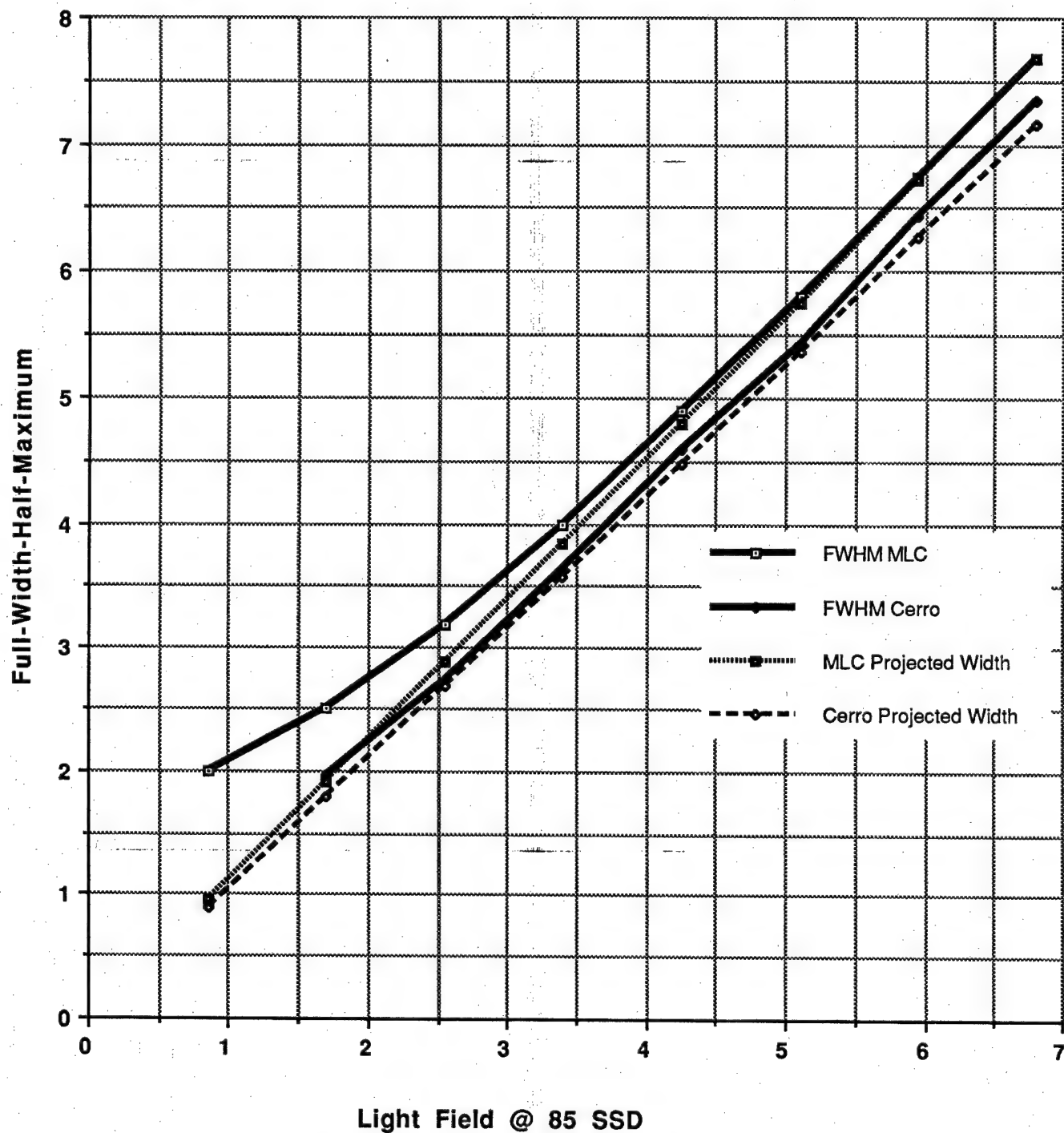


Figure 10: Comparison of 16 MeV beam profiles width vs. light field width @85 cm SSD. MLC profiles are defined by the MLC at 50.9 cm; cerrobend™ profiles are defined by the cerrobend™ aperture at 65 cm. The cerrobend™ profiles converge more rapidly to the effective width projected from the scattering foil.

### 6 MeV Relative Output vs. MLC Width Measured Data

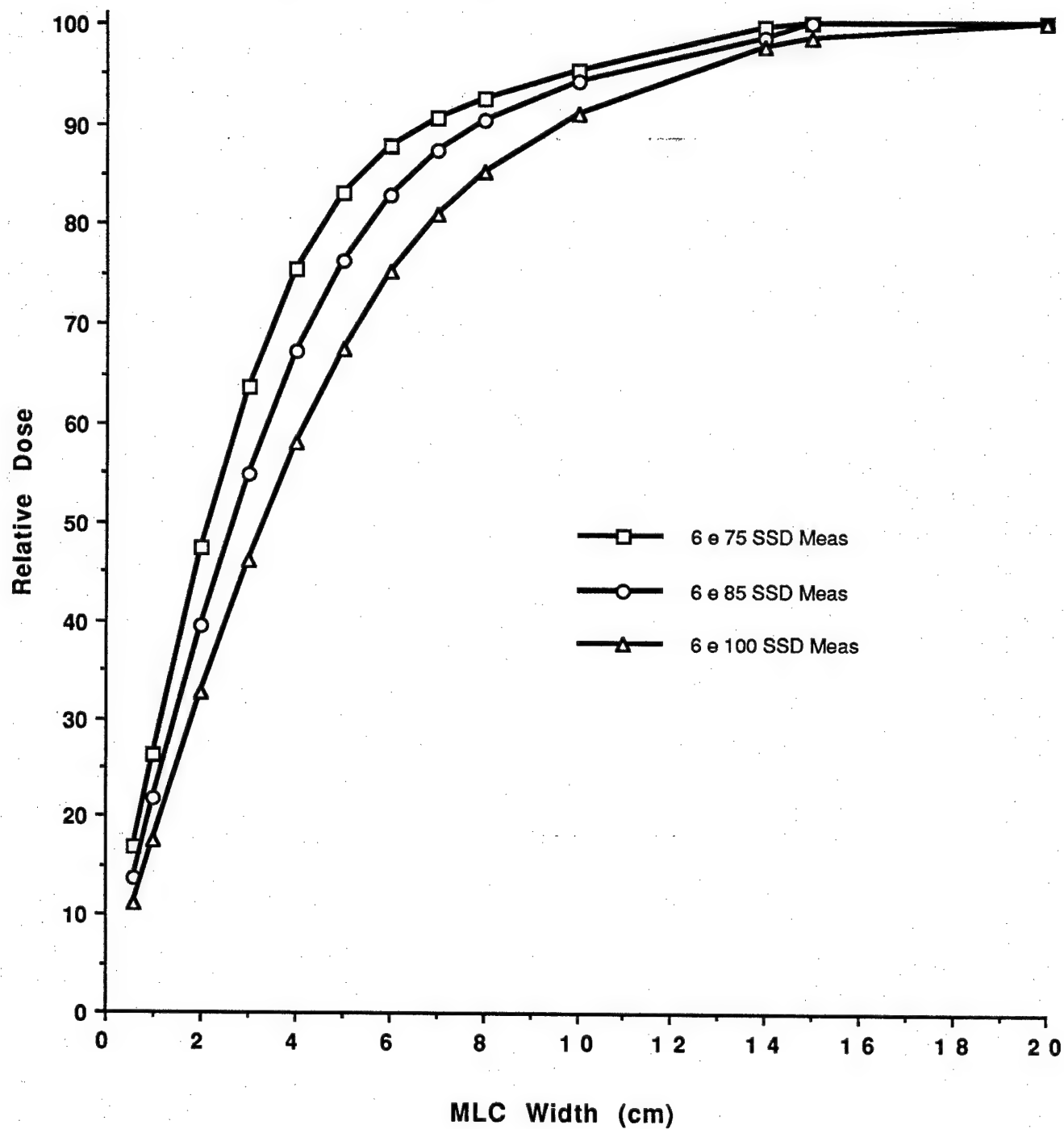


Figure 11: Measured Relative Output vs. field width and SSD.

### 6 MeV Profiles @ 85 SSD Measured vs. Monte Carlo Calculated

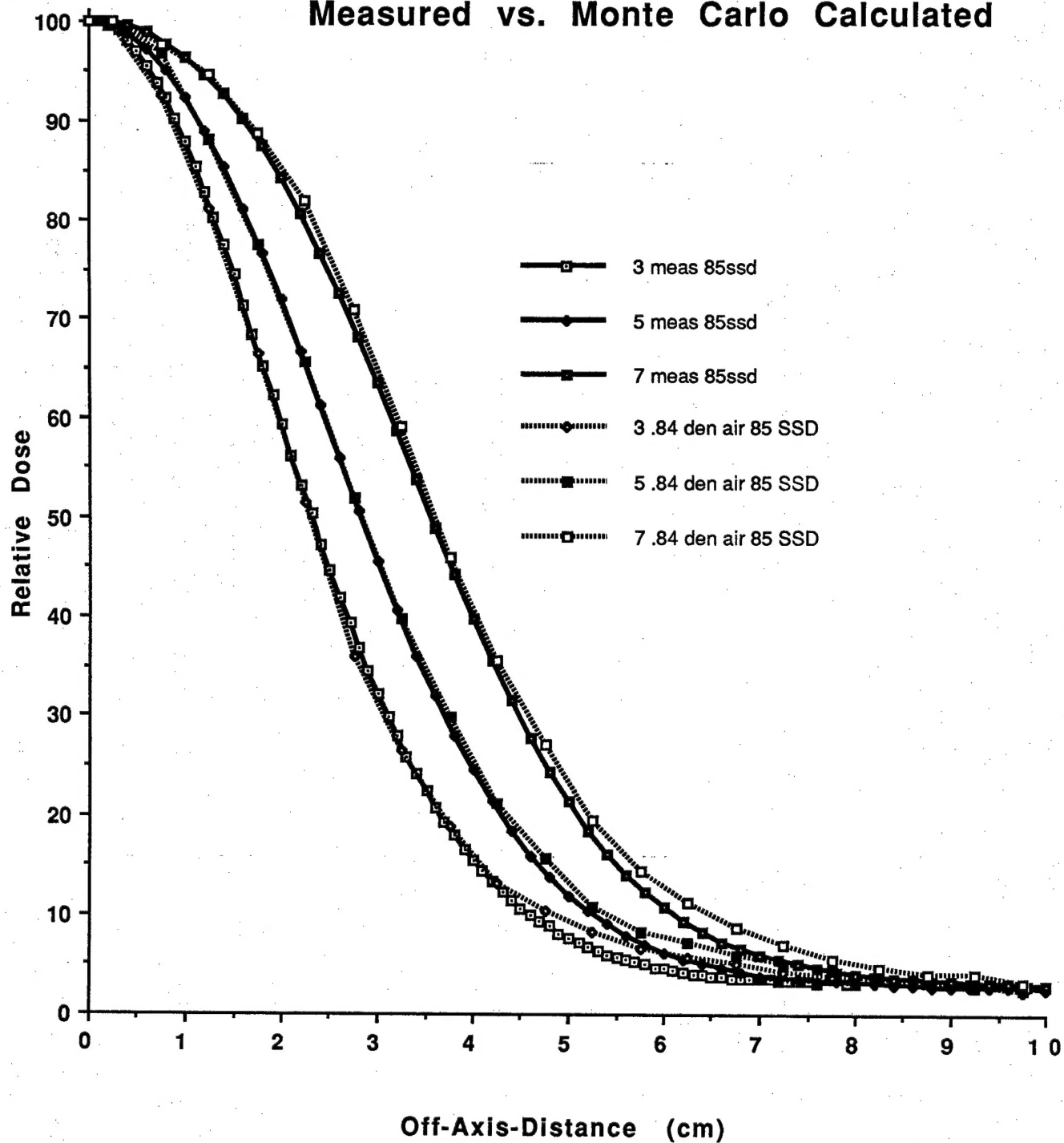


Figure 12: Monte Carlo calculated profiles for 3, 5 and 7 cm wide vs. measured data @85 cm SSD.

# 6 MeV Profiles @ 100 SSD Measured vs. Monte Carlo Calculated

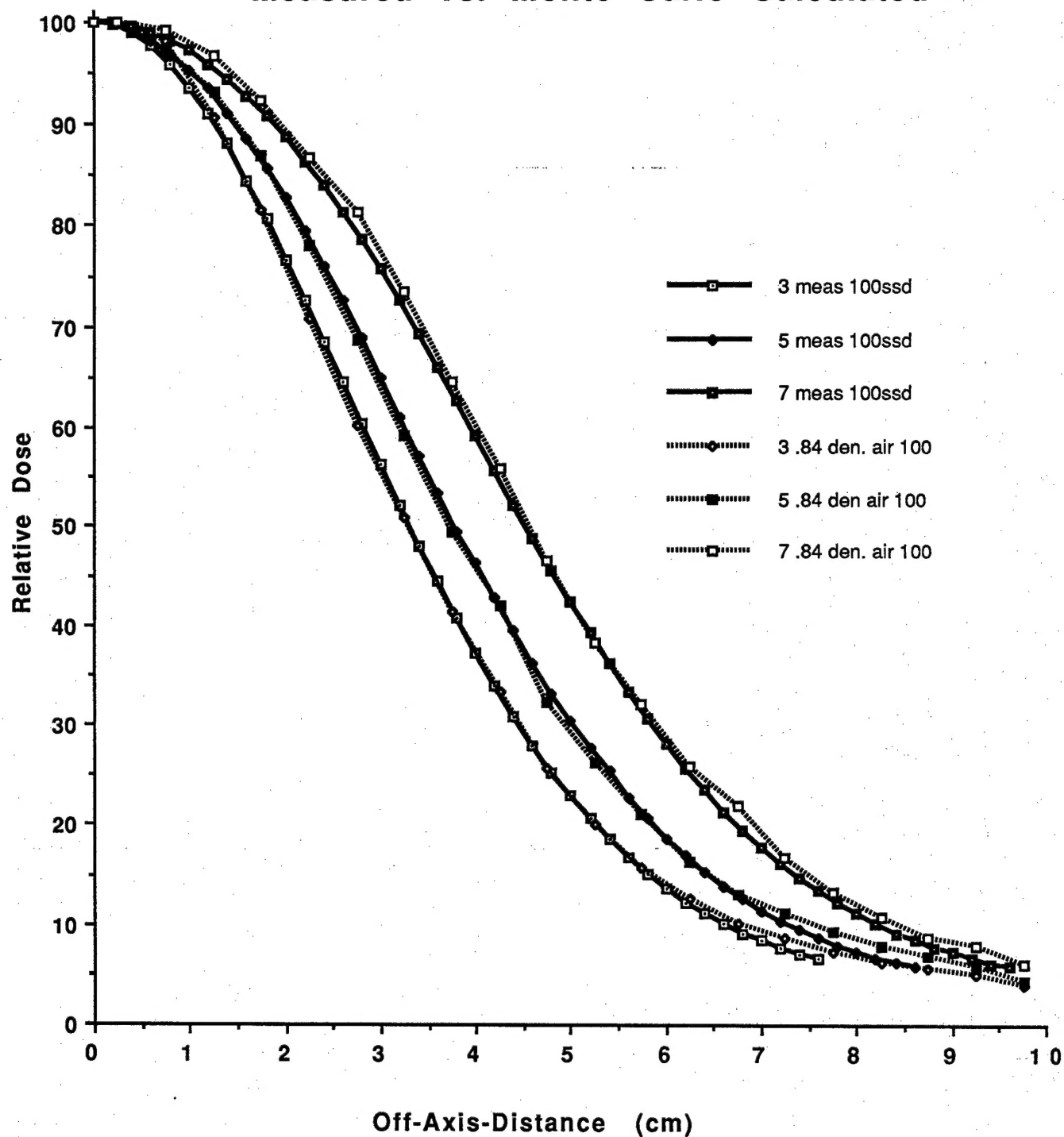


Figure 13: Monte Carlo calculated profiles for 3, 5 and 7 cm wide vs. measured data @100 cm SSD.



### Relative Output vs. MLC Width Measured vs. Monte Carlo Calculations

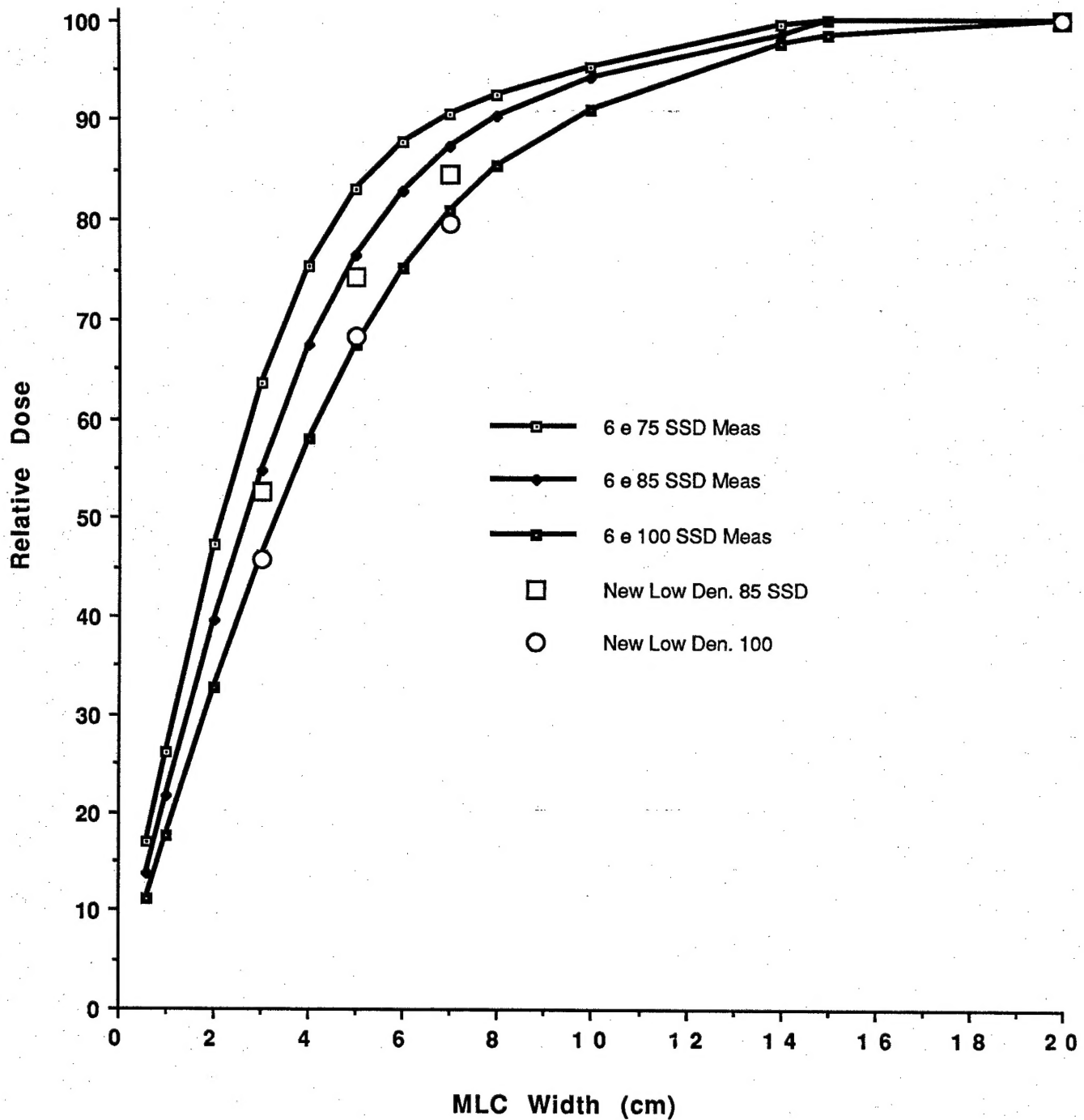


Figure 14: Monte Carlo calculated vs. measured Relative Output vs. field width and SSD.

## **KEY RESEARCH ACCOMPLISHMENTS**

- Measurement of Electron Arc Static Fields defined by Multi-Leaf Collimator
- Implementation of Monte Carlo electron dose calculation code BEAMNRC and DOSEXYZ

## **REPORTABLE OUTCOMES**

- Participant at Monte Carlo Workshop sponsored by NIH, October 2001
- Oral Presentation to be delivered at Radiological Society of North America, December 2002

## **CONCLUSIONS**

The Monte Carlo dose calculation for electrons has successfully been implemented on our computer system and will be used in an environment of 25 dedicated PC's forming a parallel calculation network. Experimental measurement of electron beam profiles for six electron energies and field widths from 1 cm to 20 cm defined by a Multi-Leaf Collimator has been completed. These measurements have been used to validate the Monte Carlo calculations of fixed-field doses. The template for a technique to optimize the dynamic MLC leaf settings during the arc in order to deliver a highly uniform dose to the postmastectomy chest wall has been defined. The dose calculations will now be integrated into the optimization program to evaluate resultant dose distributions. The work done to date is "on track" to achieve a successful completion of this project within the period of the grant.

"So What Section": The most important findings of our work to date are 1) electron arc fields can be defined using the standard Multi-Leaf Collimator; and 2) three-dimensional dose calculations using Monte Carlo techniques can successfully predict the dose distributions defined by the Multi-Leaf Collimator. These findings justify the continuing work to implement dynamic MLC electron arc therapy and to automate the process of determining the optimized collimator shapes throughout the arc. The end product of this work will be an integrated system to define treatment volume, calculate optimized dose distributions and MLC settings, and deliver the optimized dose in an efficient manner. Completion of this integrated system will enable other radiotherapy centers to implement this powerful technique for electron chest wall therapy without the labor-intensive effort previously required. Broader applications beyond chest wall therapy may include optimization of fixed electron fields using Monte Carlo simulation and intensity modulation.